UNIVERSITY OF CALIFORNIA SAN DIEGO

Mutational Study of Allostery in Receptor Protein Tyrosine Phosphatase-alpha

A Thesis submitted in satisfaction of the requirements
for the degree Master of Science

in

Biology

by

Silas Xu

Committee in charge:

Professor Nunzio Bottini, Chair
Professor Douglass Forbes, Co-chair
Professor Eric Schmelz

2022

The Thesis of Silas Xu is approved, and it is acceptable in quality and form for publication on microfilm and electronically:

University of California San Diego

2022

DEDICATION

In recognition of Dr. Nunzio Bottini for his source of knowledge, industry towards nurturing scientists, and enthusiasm for science.

TABLE OF CONTENTS

LIST OF ABBREVIATIONS

DMSO	Dimethyl sulfoxide
DiFMU	6,8-Difluoro-7-Hydroxy-4-Methylcoumarin
DiFMUP	6,8-Difluoro-4-Methylumbelliferyl Phosphate
DTT	Dithiothreitol
D1	Domain 1
D2	Domain 2
EDTA	Ethylenediamine tetraacetic acid
k_{cat}	Catalytic constant
K_M	Michaelis-Menten constant
ORF	Open Reading Frame
PTK	Protein Tyrosine Kinase
PTP domain	Phospho-Tyrosine Phosphatase domain
RPTP	Receptor Protein Tyrosine Phosphatase
Tris	tris (hydroxymethyl) aminomethane.
IPTG	isopropyl 1-thio--D-galactopyranoside
FPLC	Fast protein liquid chromatography

LIST OF FIGURES

LIST OF TABLES

ACKNOWLEDGEMENTS

I would like to acknowledge Professor Nunzio Bottini, my chair and thesis advisor, for his support by providing me with resources and guidance. His passion and dedication towards science have been motivating to me as well as other members in the laboratory. I would also like to acknowledge Dr. Eugenio Santelli for his hands-on supervision throughout the past two years. His patience and detailed advice have been indispensable to the achievement of this project.

ABSTRACT OF THE THESIS

Mutational Study of Allostery in Receptor Protein Tyrosine Phosphatase-alpha

by

Silas Xu

Master of Science in Biology

University of California San Diego, 2022

Professor Nunzio Bottini, Chair
Professor Douglass Forbes, Co-Chair

Protein Tyrosine Phosphatases (PTPs) are drug target candidates due to their role in cell signaling and involvement in the pathologies of various diseases. Difficulty in developing orthosteric inhibitors of PTPs has raised interest in the development of allosteric inhibitors. Previous studies have identified an allosteric mechanism in receptor-type protein tyrosine phosphatase α (RPTPα), yet the mechanism requires further characterization for future development of small molecule therapeutics. In this study, through comparing RPTPα and the closely related RPTPε, we achieved the identification and *in vitro* validation of a segment of RPTPα (residues 261-330) responsible for its allosteric effect. It lays the groundwork for identification of amino acid residues participating in the establishment of allostery, which is a step in fully elucidating the allosteric mechanism.

INTRODUCTION

Protein tyrosine phosphatases (PTPs) catalyze the dephosphorylation of phosphotyrosyl residues. Together with protein tyrosine kinases, they regulate many cell signaling pathways by controlling the phosphorylation states of downstream substrates (1). PTPs comprise both receptor and non-receptor members (1,2). Receptor-type protein tyrosine phosphatases (RPTPs) are defined by their transmembrane and extracellular domains and are further categorized into 8 subtypes (1,2). The R4 subtype, comprising isoforms RPTPα and RPTPε, is present in a wide variety of organisms including humans. It is characterized by having a short, highly glycosylated extracellular domain and, like most other RPTPs, a membrane-proximal intracellular catalytic domain referred to as D1, and a membrane-distal pseudo-catalytic domain referred to as D2 (Fig 1) (1,3).

RPTPα has been demonstrated to participate in the pathogenesis of a diverse range of diseases such as cancer (4), schizophrenia (5), and arthritis (6). This is unsurprising given its function in cell proliferation, differentiation, migration, cell cycle, and metabolic homeostasis, many of which are mediated through activation of Src family kinases, named after their involvement in sarcoma (1, 7). Despite PTPs being established drug targets, the search for orthosteric inhibitors (inhibitors that bind the active site of their targets) of PTPs has been hampered by poor cell permeability and target specificity of the drug candidates, due to the charged and conserved nature of the active site (8,9.) Therefore, allosteric, noncompetitive inhibitors are sought after as an alternative strategy to target RPTPα.

PTP catalysis follows a two-step mechanism. Upon substrate binding (k_1), the nucleophilic cysteine (C433 in RPTPα, Fig 1B) attacks the phosphate group, forming a phosphocysteine intermediate and releasing the tyrosyl leaving group (k_2). The aspartic acid

residue in the WPD loop (W399-D401 in RPTPα) facilitates the tyrosyl dissociation by protonating the oxygen. In the second step, this aspartate deprotonates a water molecule, which attacks and breaks down the phosphocysteine intermediate (k_3) (3, 10).

A previous study in our laboratory reported the crystal structure of the RPTPα tandem cytoplasmic domains (PDB: 6UZT) and unraveled an allosteric mechanism of D2 on its phosphatase activity (3). D2 was shown to restrict the function of the catalytically prominent WPD loop by interacting with the $P^{405}FTP^{408}$ motif at the interface between the two domains (Fig 1B) (10, 11). This mechanism could be disrupted by mutating F406 and T407 to alanines (FATA). However, this allosteric mechanism is surprisingly absent in RPTPε, which shares with RPTPα 70% of sequence identity in the intracellular domains (3). The detailed analysis of the differences between the two isoforms may provide further insight into this mechanism and potentially lead to future discovery of allosteric inhibitors for RPTPα. Here, through kinetic analysis of RPTPα/ε chimeras generated by subcloning corresponding segments of RPTP α and ε into each other, we demonstrate that an N-terminal segment of D1 (residue 263-330) is a component of this allosteric mechanism.

MATERIALS & METHODS

Subcloning and site-directed mutagenesis

All mutants and chimeras were generated using pET28 plasmids containing codon-optimized ORFs encoding the intracellular domains of RPTPα (residues 202-793) or RPTPε (residues 104-699) (GenScript). Both ORFs contain 11 unique, matching restriction sites for subcloning and a C-terminal six-histidine tag. The plasmids were digested with selected restriction enzymes (New England Biolabs). The resulting fragments were separated by agarose gel electrophoresis, extracted with a QIAquick Gel Extraction Kit, (QIAGEN) and religated with T4 DNA ligase (New England Biolabs) to generate the desired chimeras. Site-directed mutagenesis was performed by polymerase chain reactions (PCR) with Pfu polymerase (Agilent Technologies). All primers were synthesized by Integrated DNA Technologies. The PCR products were purified with QIAquick PCR Purification Kit (QIAGEN, digested with DpnI (New England Biolabs), and transformed into E. coli XL10. All constructs were sequenced to confirm the desired sequence.

Protein expression and purification

Plasmids containing the desired ORFs were transformed into E. coli BL21(DE3) and grown on LB-agar plates containing 50 μg/mL kanamycin. Individual colonies were inoculated to 5 mL of LB medium. These starting cultures were then diluted 1:1000 in LB medium and grown in a shaker flask at 37□ until the OD reached ~0.6. Protein expression was induced by 0.5 mM isopropyl 1-thio--D-galactopyranoside (IPTG) for >12h at room temperature. Cells were harvested by centrifuging at 8000 rpm for 8 minutes. The supernatant was removed and the pellets were resuspended in 300 mM NaCl, 20 mM Tris (pH 7.9). Cells were then lysed with lysozyme (0.1 mg/ml; Thermo Fisher Scientific) by flash freezing in liquid nitrogen and thawing (12). The lysates were treated with DNase I (1 mg/ml; Roche) and centrifuged at 14500 rpm for 60 minutes. Proteins were purified from the soluble fraction of the lysate by gravity-flow affinity chromatography with Ni-NTA Agarose (Qiagen),

followed by dialysis and anion-exchange Fast-Protein Liquid Chromatography (FPLC) using a NGC 10 Medium-Pressure Chromatography Systems (Bio-Rad) and a POROS 20 HQ column (Thermo Fisher Scientific) (3).

Phosphatase activity assays

Proteins were diluted to 2 nM in 2x T1 buffer [100 mM Tris (pH 7.3), 20mM DTT, 0.02% Triton-X100]. The synthetic phosphatase substrate, 6,8-difluoro-4-methylumbelliferyl phosphate (DiFMUP, Invitrogen) was prepared to a series of concentrations (800, 400, 200, 80, 40, 20, 8, and 0 μM) in 8% DMSO. For proteins with higher K_M values (> 50 μM), DiFMUP concentrations were doubled. After loading samples into a 96-well black polystyrene microplate (Corning), the plate was warmed to 37□. Then, 25 μl of protein and DiFMUP solutions were mixed. The fluorescence of the dephosphorylated product, DiFMU, produced was continuously measured by a Tecan Infinite 200 plate reader for 10 minutes at 358 nm excitation and 455 nm emission wavelength. In order to convert fluorescence intensity to DiFMU concentration, a series of calibrations were performed for each concentration by combining known amounts of DiFMUP and DiFMU in assay buffer. Initial reaction rates were obtained by linear regression and fitted to a Michaelis-Menten curve by non-linear regression in Graphpad PRISM 7 to yield the Michaelis-Menten parameters.

RESULTS

Comparison between the crystal structures of RPTPα (6UZT) and RPTPε (2JJD) had previously shown that the interdomain angle between D1 and D2 of RPTPε was larger than that of RPTPα by approximately 18° (Fig 1A) (3). We speculated that RPTPε with a larger degree of interdomain separation or increased flexibility accounts for its lack of domain D1 allosteric control by domain D2 (Fig 1A) (3). We initially hypothesized that the amino acid residues close to the D1-D2 interface were more likely to affect the interdomain separation or flexibility and therefore had a higher probability of being part of the RPTPα allosteric mechanism (Fig 1B). We also explored the hypothesis that the steric repulsion between L450 and H492 in RPTPα could be stronger than that between M352 and Y394 in RPTPε due to the additional constraints imposed by the leucine branched side chain, resulting in different degrees of rotation along the hypothesized axis (Fig 1A).

Towards these goals, we generated a mutant containing a series of substitutions at the interface in RPTPα to the corresponding residues in RPTPε. The mutant protein contained the mutations N222R, R223I, M225S, N229C, V483T, S533N, I534V, K535R, Q537M, N538K, D539E, and K540N, as well as L450M and H492Y. It is referred to as the "RPTPα Interface mutant" or "RPTPα INT" (Fig 1). The aforementioned FATA mutation was used as a control where the allostery in RPTPα was disrupted.

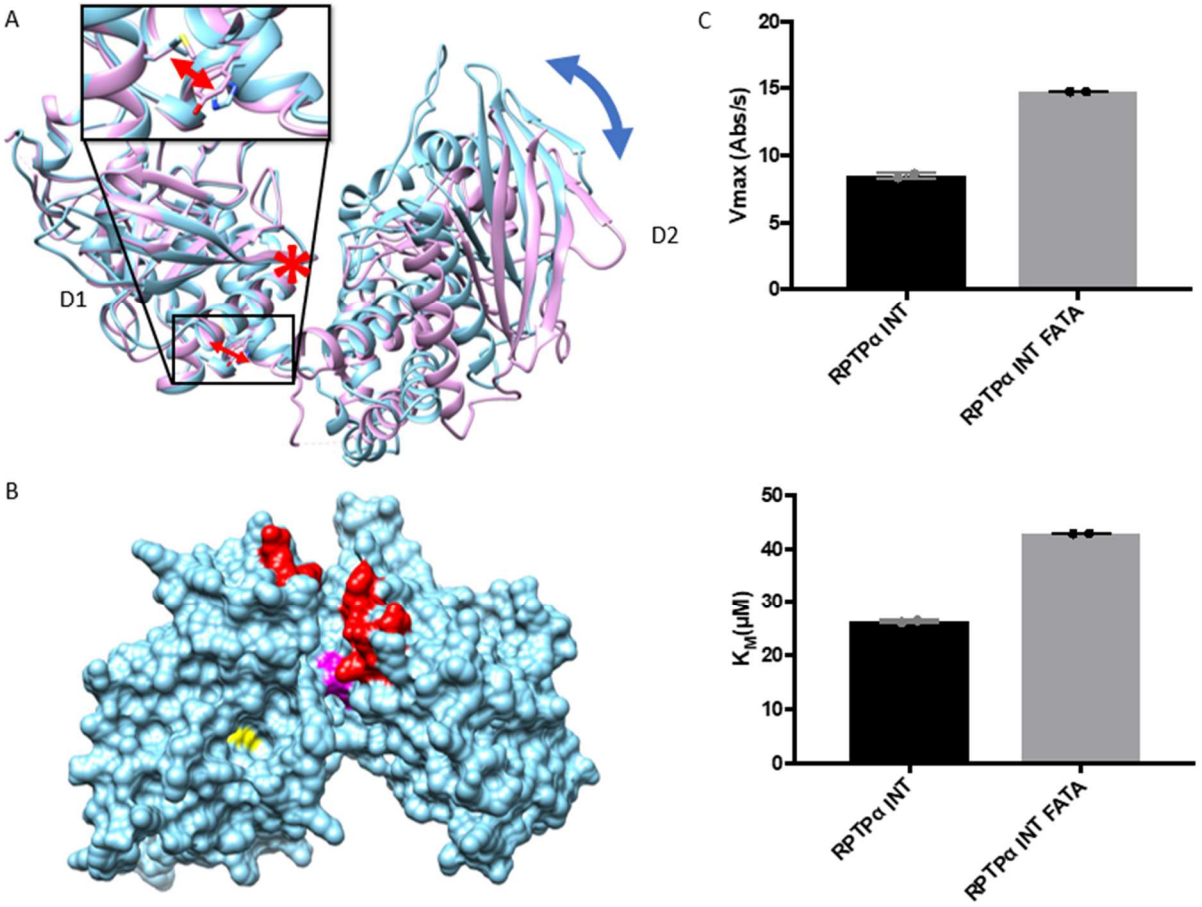

Figure 1. Preliminary Data of RPTPα Interface mutant. (A) Ribbon representation of RPTPα (blue) and RPTPε (pink) with superimposed D1s and a detail of areas surrounding L450 and H492 (α) or M352 and Y394 (ε). Red arrows represent hypothesized repulsion between the two residues. The asterisk represents the approximate axis of rotation that brings D2s into superposition if D1s are fixed in place. Blue arrows show the different orientation of D2s in the two RPTPs. (A) Solvent-accessible surface representation of RPTPα. Amino acid residues mutated in the interface mutant are colored in red. Active-site cysteine (C433) is colored in yellow; F406 and T407 are colored in magenta. (C) Bar graphs showing preliminary V_{max} and K_M for each of the mutants above. Each data point represents one individual experiment with three technical replicates (n=3) and error bar represents standard deviation.

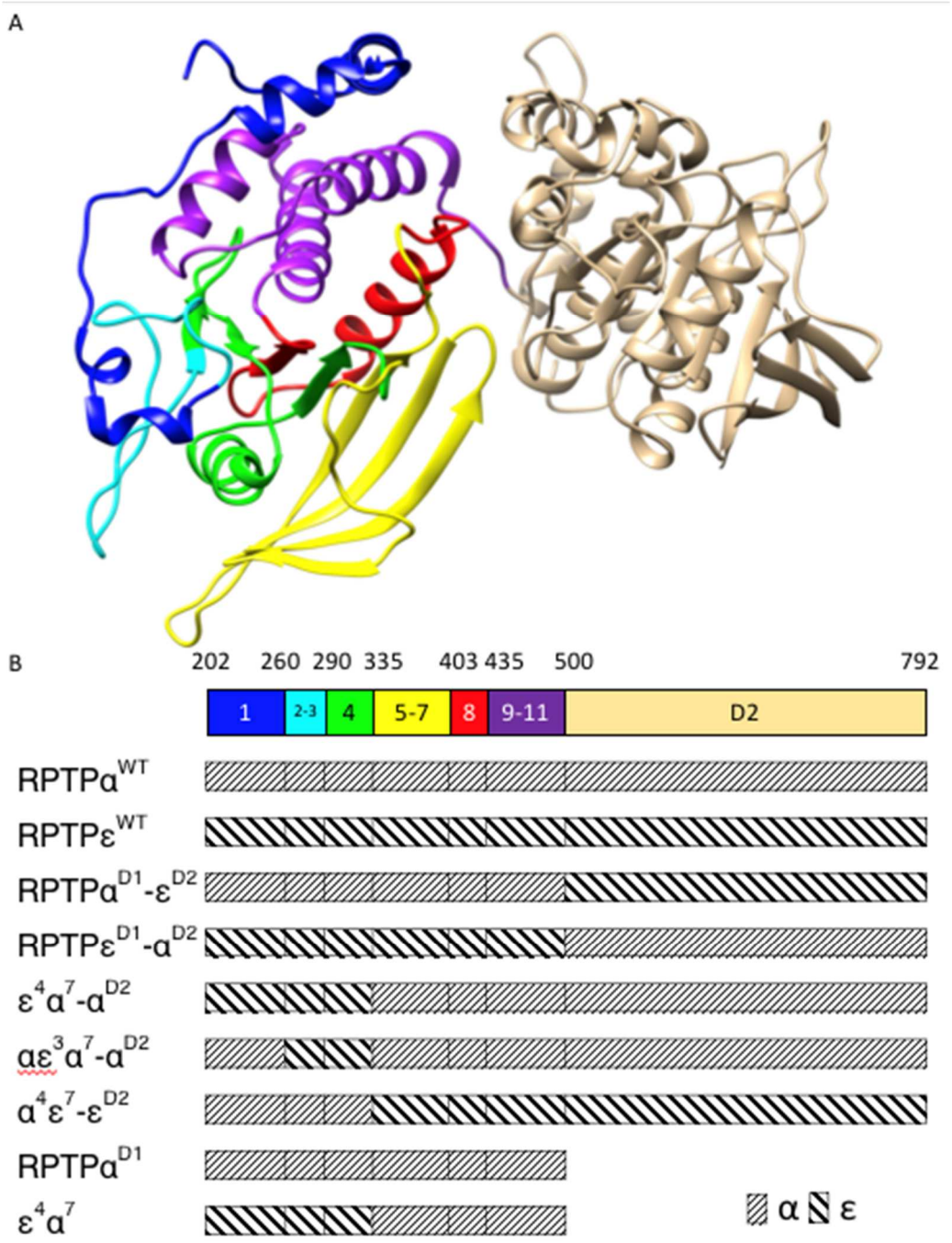

Figure 2. Graphic and sequential maps of segments used in this study. (A) Ribbon representation of RPTPα, with sequence segments divided by restriction sites shown in different colors. Some segments are combined for visual clarity. (B) Linear map of segments in (A) and description of chimeras used in this study. Thin lines, α. Think lines, ε.

Purified RPTPα INT and RPTPα INT^{FATA} phosphatase proteins were produced and assayed for their activity on DiFMUP. We have previously noted that inhibition of activity of RPTPα by the D2 domain is characterized by a decrease in both k_{cat} and K_M when using DiFMUP (3). According to our preliminary data here, RPTPα INT displayed significantly lower V_{max} and K_M compared to RPTPα INT^{FATA}, suggesting that the activity of RPTPα INT is still inhibited by D2. (Fig 1C). Therefore, we conclude that none of the mutations in RPTPα INT significantly disrupt the allosteric effect.

The lack of effect produced by the rationally designed mutant set approach described above led us to next take a grouped screening approach. For this, we generated the domain swapping chimeras RPTPα^{D1}-ε^{D2} and RPTPε^{D1}-α^{D2}, a strategy used in previous studies by the Deane group (Fig 2,3) (13). It is worth noting that both human and mouse RPTPε were used to generate chimeras with human RPTPα, but the chimeras with mRPTPε were only used for preliminary data. In this domain swapping approach, we observed a significant increase in turnover number (k_{cat}) in both hRPTPα^{D1}-ε^{D2FATA} and hRPTPε^{D1}-α^{D2FATA} as compared to the corresponding wild-type proteins; that is, both chimeras displayed the α-like behavior of allosteric repression. In contrast, unlike for normal RPTPα, the K_Ms of both chimeras were similar to those of their respective FATA mutants (ε-like behavior) (Fig 3A, Table 1). In other words, while neither D1 nor D2 alone are sufficient to confer α-like characteristics with respect to K_M, both are individually capable of inducing it with respect to k_{cat}. However, preliminary data had previously shown little difference between RPTPmε^{D1}-hα^{D2} and RPTPmε^{D1}-hα^{D2FATA}, indicating that whether the protein had either α- or ε-like behavior was primarily determined by D1. (Fig 3B). Given the 95% identities and 98% positives between human and mouse RPTPε, focusing on the apparent differences between the D1s of human and mouse RPTPε may provide future insights regarding the allosteric mechanism.

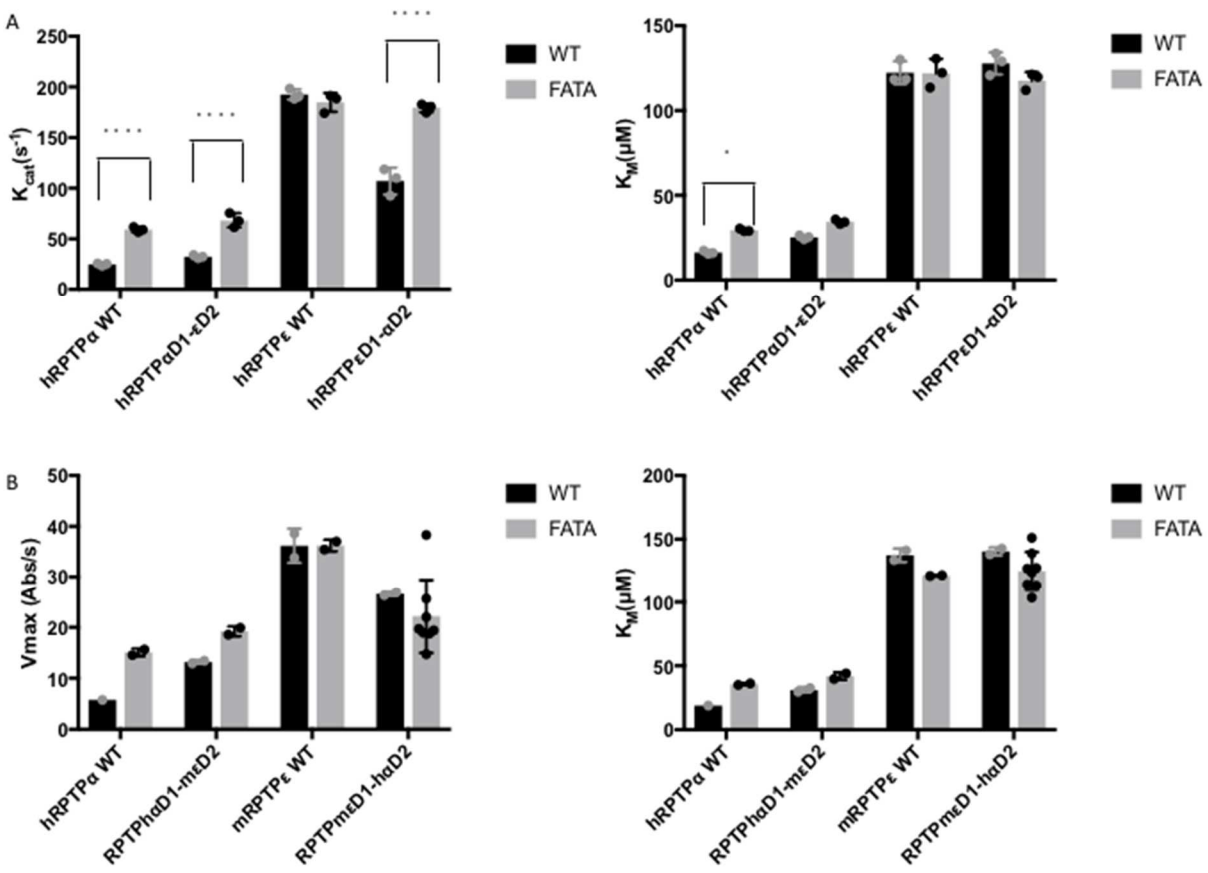

Figure 3. RPTPα/ε differ in interdomain angle and allosteric behavior. (A) Bar graphs showing k_{cat} and K_M of domain-swapping mutants between human RPTPα and RPTPε. Each data point represents one individual experiment for which Michaelis–Menten parameters were calculated by averaging three technical replicates. Error bars, S.D. A two-way ANOVA test was used. (*, $p < 0.05$. ****, $p < 0.0001$) (B) Bar graphs showing preliminary V_{max} and K_M of domain-swapping mutants between hRPTPα and mRPTPε. Each data point represents one individual experiment for which Michaelis–Menten parameters were calculated by averaging three technical replicates. Error bars, S.D.

Table 1. Michaelis-Menten parameters for all proteins mentioned. k_{cat} values are in s^{-1}, K_M in µM. Values are mean ± SD of three independent experiments.

Name	k_{cat}	K_M	k_{cat} of FATA mutant	K_M of FATA mutant	$k_{cat}^{FATA}/K_{cat}^{WT}$
RPTPα^{WT}	24.8 ± 1.2	16.3 ± 1.0	59.2 ± 2.4	29.5 ± 0.8	2.39 ± 0.21
RPTPε^{WT}	192.7 ± 5.1	122.4 ± 6.7	184.8 ± 9.2	122.1 ± 8.5	0.96 ± 0.10
RPTPα^{D1}	42.4 ± 2.1	24.6 ± 0.3	62.3 ± 3.0	32.8 ± 0.3	1.50 ± 0.14
RPTPα^{D1}-ε^{D2}	32.5 ± 1.6	25.3 ± 1.1	68.3 ± 7.0	34.5 ± 1.3	2.10 ± 0.32
RPTPε^{D1}-α^{D2}	107.1 ± 13.3	127.8 ± 6.5	179.4 ± 4.2	117.7 ± 4.9	1.68 ± 0.25
$\varepsilon^4\alpha^7$-α^{D2}	**117.9 ± 2.6**	**123.9 ± 2.7**	**176.3 ± 8.5**	**135.4 ± 2.0**	**1.50 ± 0.11**
$\alpha\varepsilon^3\alpha^7$-$\alpha^{D2}$	**138.9 ± 4.8**	**169.9 ± 5.6**	**188.2 ± 14.1**	**191.2 ± 43.8**	**1.35 ± 0.15**
$\varepsilon^4\alpha^7$	156.1 ± 11.2	121.3 ± 6.0	191.9 ± 9.1	112.4 ± 6.8	1.23 ± 0.15
$\alpha^4\varepsilon^7$-ε^{D2}	118.8 ± 4.0	56.0 ± 0.4	155.7 ± 1.2	63.9 ± 0.4	1.31 ± 0.05

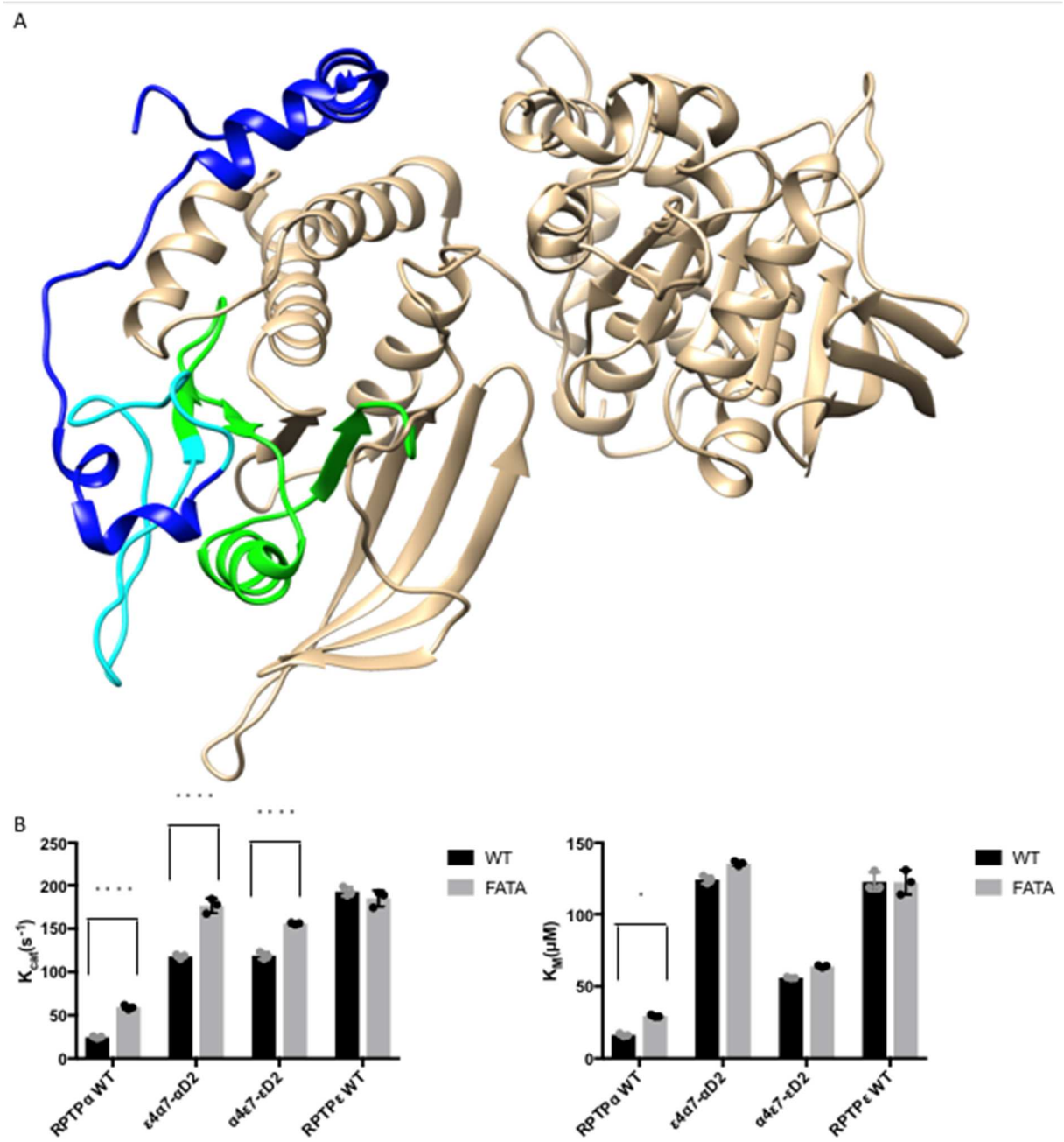

Figure 4. RPTPα residues 202-330 are a component of the allosteric mechanism by D2 domain. (A) Ribbon representation of $\varepsilon^4\alpha^7$-α^{D2} or $\alpha^4\varepsilon^7$-ε^{D2}. The color scheme is the same as Figure 2. (B) Bar graphs showing k_{cat} and K_M of the phosphatase mutants. Each data point represents one individual experiment with three technical replicates (n=3) and error bar represents standard deviation. A two-way ANOVA test was used. (*, $p < 0.1$. ****, $p < 0.0001$)

We next sought to investigate the roles of specific amino acid regions affecting this allosteric mechanism, focusing on D1. Within D1, 10 unique restriction sites were encoded in the homologous sequences between RPTPα and RPTPε, allowing the sequences in between to be exchanged by subcloning. Therefore, the restriction sites divided the D1s into 11 swappable, sequential segments, with D2 being another segment (Fig 2). We decided to specifically investigate segments 1-4, 5-7, and 8-11. Chimeras were generated by substituting the above-mentioned segment groups from RPTPε into RPTPα. Preliminary data suggested that all three chimeras showed less increase in K_M upon FATA mutation to various degrees. Construct $\varepsilon^4\alpha^7$-α^{D2FATA} (RPTPα with the 4 N-terminal segments substituted with those from RPTPε) showed a ~1.5-fold increase in kinetic activity compared to $\varepsilon^4\alpha^7$-α^{D2} (Fig 4, Table 1). Therefore, $\varepsilon^4\alpha^7$-α^{D2} shows a behavior more similar to RPTPα^{D1} than to RPTPα^{WT}, which displayed 1.5-fold and 2.4-fold elevation in reaction rate upon FATA mutation, respectively (Fig 4, 5, Table 1) (3). Since the allosteric behavior is not present in RPTPα^{D1} due to the lack of D2, the similar elevation of k_{cat} between $\varepsilon^4\alpha^7$-α^{D2} and RPTPα^{D1} upon FATA mutation indicated that the allostery was partially disrupted in $\varepsilon^4\alpha^7$-α^{D2}.

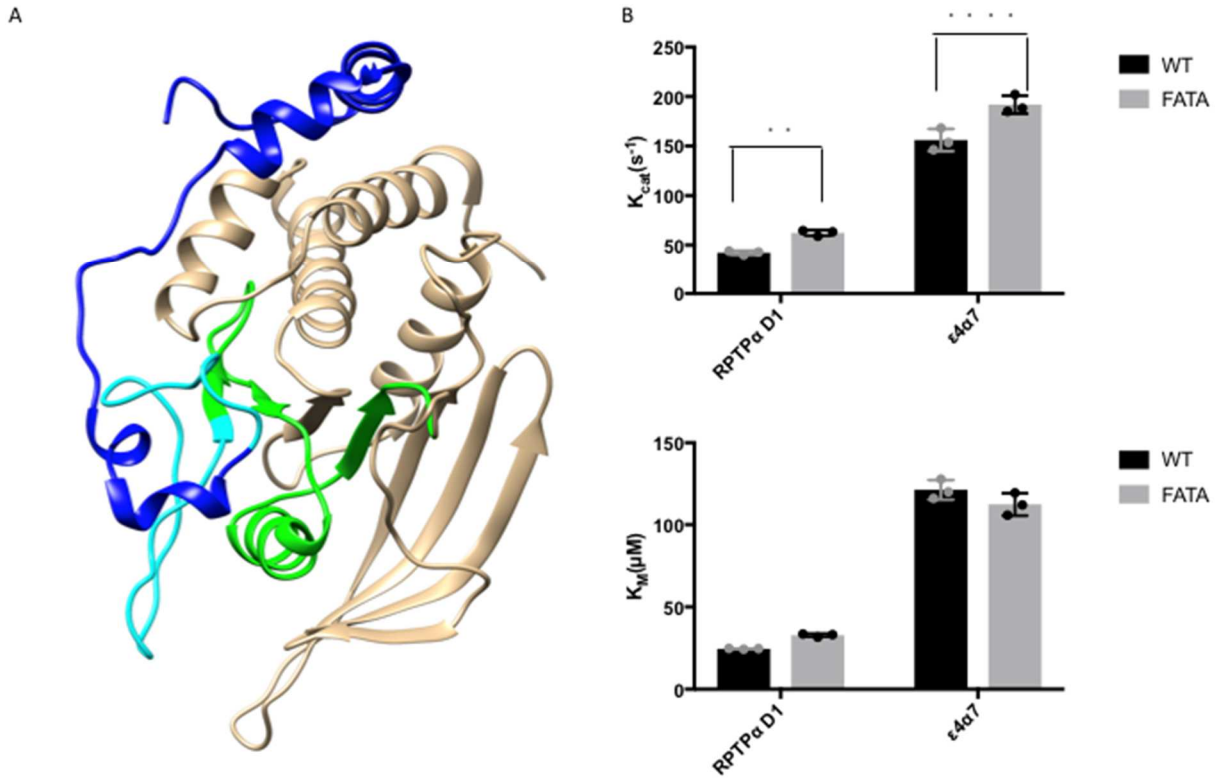

Figure 5. Validation of results with D1 mutants. (A) Ribbon representation of $\varepsilon^4\alpha^7$. The color scheme is the same as Figure 2. (B) Bar graphs showing k_{cat} and K_M of the D1 mutants. Each data point represents one individual experiment with three technical replicates (n=3) and error bar represents standard deviation. A two-way ANOVA test was used. (**, $p < 0.01$. ****, $p < 0.0001$)

To further investigate the effects of swapping the four N-terminal segments from RPTPε into RPTPα, D2 was deleted from $\varepsilon^4\alpha^7$-α^{D2} to generate $\varepsilon^4\alpha^7$. As expected, $\varepsilon^4\alpha^{7FATA}$ displayed a ~1.2x higher k_{cat} than $\varepsilon^4\alpha^7$, similar to RPTPα^{D1}, suggesting lack of allosteric control (Fig 5, Table 1). The smaller effect of FATA mutation on $\varepsilon^4\alpha^7$ than $\varepsilon^4\alpha^7$-α^{D2} also supported the idea that the allostery was only partially disrupted in $\varepsilon^4\alpha^7$-α^{D2}. We then attempted to engineer the allosteric mechanism in RPTPε by swapping in the same segments from RPTPα. The resulting $\alpha^4\varepsilon^7$-ε^{D2FATA} showed only a moderately higher k_{cat} (~1.3x) compared to that of $\alpha^4\varepsilon^7$-ε^{D2}. (Fig 4, Table 1) Although the FATA mutation affected the catalytic activity of $\alpha^4\varepsilon^7$-ε^{D2}, the effect was small compared to that on RPTPα^{WT}. Thus, the allosteric mechanism of RPTPα was not reintroduced in $\alpha^4\varepsilon^7$-ε^{D2}, suggesting the involvement of regions outside of the N-terminal segments. Attempts were also made to further pinpoint the amino acids involved in the allosteric behavior from the N-terminal region. We generated chimera $\alpha\varepsilon^3\alpha^7$-$\alpha^{D2}$ and $\alpha\varepsilon^3\alpha^7$-$\alpha^{D2FATA}$. Interestingly, the $\alpha\varepsilon^3\alpha^7$-$\alpha^{D2}$ WT/FATA construct behaved similarly to the $\varepsilon^4\alpha^7$-α^{D2} as well as hRPTPε^{D1}-α^{D2} construct (Fig 6, Table 1), suggesting that similar effects regarding the allostery were achieved by substituting the entire D1 domain, the four N-terminal segments, or the 2nd to 4th segments from RPTPε into RPTPα. Therefore, the allosteric control was disrupted in $\alpha\varepsilon^3\alpha^7$-$\alpha^{D2}$ to a similar degree as $\varepsilon^4\alpha^7$-α^{D2} and hRPTPε^{D1}-α^{D2}.

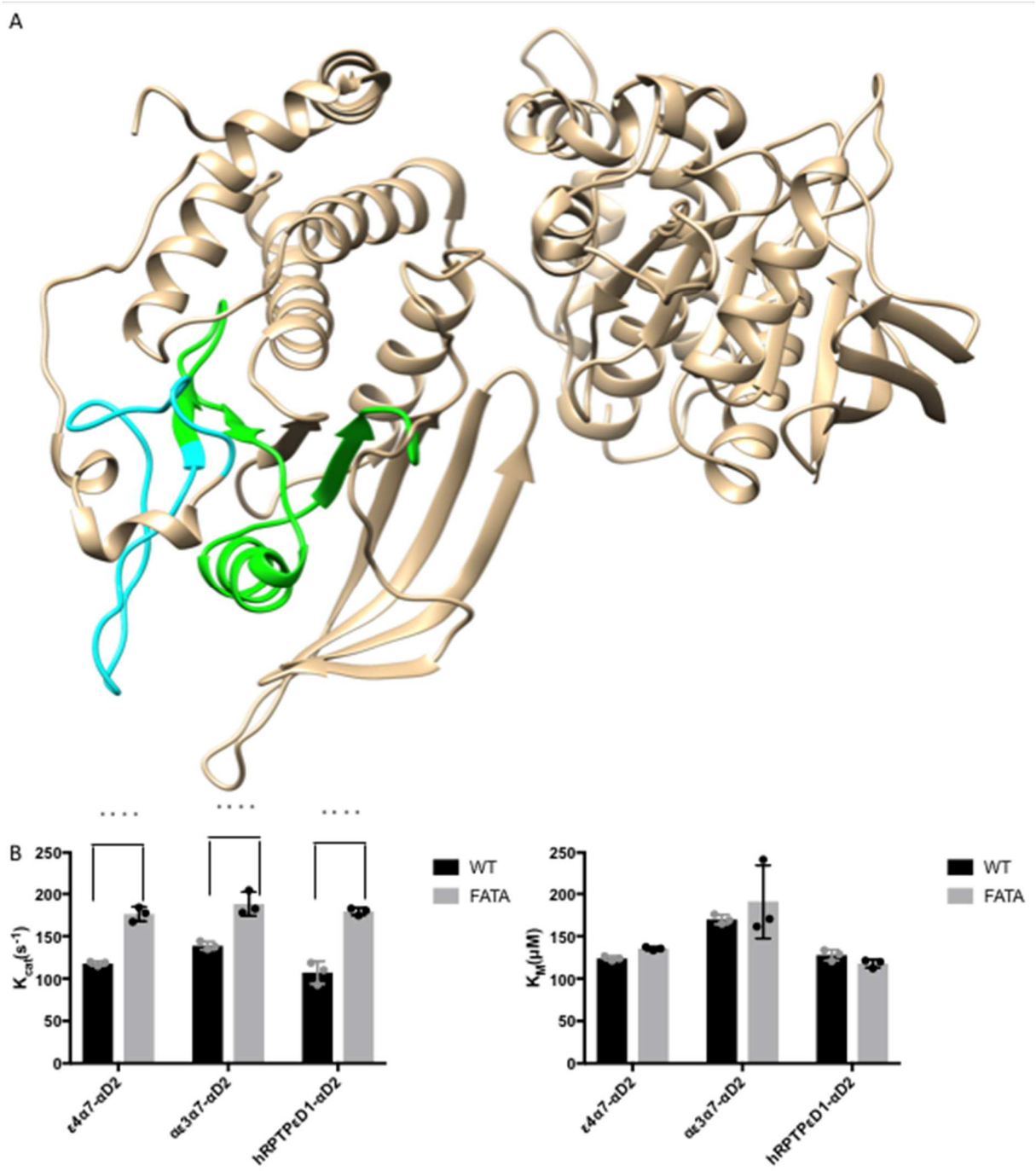

Figure 6. RPTPα residues 261-330 are a component of the allosteric mechanism by D2 domain. (A) Ribbon representation of $\alpha\varepsilon^3\alpha^7$-$\alpha^{D2}$. The color scheme is the same as Figure 2. (B) Bar graphs showing k_{cat} and K_M of the phosphatase mutants. Each data point represents one individual experiment with three technical replicates (n=3) and error bar represents standard deviation. A two-way ANOVA test was used. (****, $p < 0.0001$)

DISCUSSION

Due to the importance of PTPs in signal transduction and the difficulties of finding orthosteric inhibitors, allosteric regulation in PTPs has been under investigation for the possibility of identifying druggable sites as well as modulators. In this study, we took advantage of the high conservation but divergent allosteric behaviors between RPTPα and RPTPε to study the allosteric mechanism in RPTPα. In the first approach, we rationally selected and mutated a large number of amino acids that differ between RPTPα and RPTPε, focusing on the ones near the D1-D2 interface (Fig 1). However, this mutated version retained the allosteric behavior, indicating that these amino acids were not the ones involved. In our second approach, through swapping different segments between RPTPα and RPTPε, we found the region spanning the 2nd to 4th segments (residues 263-330 in RPTPα) to potentially contain one or more amino acid residue(s) that are essential for the establishment of allosteric behavior, since the swap caused a decrease in allostery. However, this 2nd to 4th segment region still contains 17 non-conserved residue pairs between RPTPα and RPTPε, and further screening would be necessary for the elucidation of the allosteric mechanism. Out of all the non-conserved amino acid pairs, 11 belong to the same category as one another (polar, aliphatic, aromatic, positively charged, negatively charged), and thus are less likely to account for the difference between the two RPTPs. It is worth noting that 3 of the 6 different residue pairs (H274-I177, P277-Q180, and D283-C186) are located close together on the same loop, making this cluster a good target for further investigation. Interestingly, this cluster is located near the outer edge of D1 and very far from the D1-D2 interface, which would contradict our initial hypothesis that amino acid residues close to the interface had a higher probability of affecting the allosteric control.

Future work could follow a number of potentially revealing avenues. One limitation of this study was that DiFMUP was the only phosphatase substrate used. Phosphatase activity assays with other substrates could potentially help validate the results, especially when results from DiFMUP assays had larger variances. Also, substrates involving different dephosphorylation mechanisms may

offer additional insights regarding the properties of the mutants. For example, comparing kinetic parameters using DiFMUP and the closely related 4-methylumbelliferyl phosphate (MUP) would potentially yield interesting observations. This is because of the low pK_a (4.7 vs 7.8) of the product of DiFMUP hydrolysis, DiFMU, compared to that of MU, which allows dephosphorylation without requiring acid catalysis and, therefore, WPD loop involvement. As a result, when using DiFMUP, k_{cat}/K_M [which equals $k_2 \cdot k_1/(k_2+k_{-1})$], is only dependent on the kinetics of substrate binding (k_1 and k_{-1}) and would not be affected by the FATA mutation, making k_{cat} and K_M move in the same direction (3). Here, since $\alpha\varepsilon^3\alpha^7$-$\alpha^{D2}$ and $\varepsilon^4\alpha^7$-α^{D2} displayed significant increases in k_{cat} [$= k_2 \cdot k_3 / (k_2+k_3)$] but not K_M upon FATA mutation, it could be inferred that the FATA mutation affects catalysis by more than merely relaxing restrictions on WPD loop motions. Another potential avenue is that only a small portion of the possible chimeras were generated by us during this study. Future different combinations of segments may be useful for establishing correlations between certain segments and the presence/absence of allosteric behavior. In addition, a similar methodology can be used for identifying relevant regions in D2.

In conclusion, this study lays the foundation for unraveling the allosteric mechanism of RPTPα and potentially other Protein Tyrosine Phosphatases. Here we have identified D1 segment 2-4 of RPTPα as likely containing one or more amino acid residues that are essential component(s) of the allosteric mechanism of RPTPα.

REFERENCES

1. Tonks, N. K. Protein Tyrosine Phosphatases: From Genes, to Function, to Disease. Nature Reviews Molecular Cell Biology 2006, 7 (11), 833–846.

2. Alonso, A.; Sasin, J.; Bottini, N.; Friedberg, I.; Friedberg, I.; Osterman, A.; Godzik, A.; Hunter, T.; Dixon, J.; Mustelin, T. Protein Tyrosine Phosphatases in the Human Genome. Cell 2004, 117 (6), 699–711.

3. Wen, Y.; Yang, S.; Wakabayashi, K.; Svensson, M. N. D.; Stanford, S. M.; Santelli, E.; Bottini, N. RPTPα Phosphatase Activity Is Allosterically Regulated by the Membrane-Distal Catalytic Domain. Journal of Biological Chemistry 2020, 295 (15), 4923–4936.

4. Du, Y.; Grandis, J. R. Receptor-Type Protein Tyrosine Phosphatases in Cancer. Chinese Journal of Cancer 2015, 34 (2), 61–69.

5. John, J.; Kukshal, P.; Sharma, A.; Bhatia, T.; Nimgaonkar, V. L.; Deshpande, S. N.; Thelma, B. K. Rare Variants in Protein Tyrosine Phosphatase, Receptor Type A (PTPRA) in Schizophrenia: Evidence from a Family Based Study. Schizophrenia Research 2019, 206, 75–81.

6. Stanford, S. M.; Svensson, M. N.; Sacchetti, C.; Pilo, C. A.; Wu, D. J.; Kiosses, W. B.; Hellvard, A.; Bergum, B.; Muench, G. R.; Elly, C.; Liu, Y.-C.; den Hertog, J.; Elson, A.; Sap, J.; Mydel, P.; Boyle, D. L.; Corr, M.; Firestein, G. S.; Bottini, N. Receptor Protein Tyrosine Phosphatase α-Mediated Enhancement of Rheumatoid Synovial Fibroblast Signaling and Promotion of Arthritis in Mice. Arthritis & Rheumatology 2016, 68 (2), 359–369.

7. Roskoski, R. Src Kinase Regulation by Phosphorylation and Dephosphorylation. Biochemical and Biophysical Research Communications 2005, 331 (1), 1–14.

8. Stanford, S. M.; Bottini, N. Targeting Tyrosine Phosphatases: Time to End the Stigma. Trends in Pharmacological Sciences 2017, 38 (6), 524–540.

9. Zhang, Z.-Y. Drugging the Undruggable: Therapeutic Potential of Targeting Protein Tyrosine Phosphatases. Accounts of Chemical Research 2016, 50 (1), 122–129.

10. Zhang, Z.-Y. Mechanistic Studies on Protein Tyrosine Phosphatases. Progress in Nucleic Acid Research and Molecular Biology 2003, 171–220.

11. Pannifer, A. D. P.; Flint, A. J.; Tonks, N. K.; Barford, D. Protein Tyrosine Phosphatase 1B Cysteinyl-Phosphate Intermediate. 1998.

12. Ron, E. Z.; Kohler, R. E.; Davis, B. D. Polysomes Extracted from Escherichia Coli by Freeze-Thaw-Lysozyme Lysis. Science 1966, 153(3740), 1119–1120.

13. Hay, I. M.; Fearnley, G. W.; Rios, P.; Köhn, M.; Sharpe, H. J.; Deane, J. E. The Receptor PTPRU Is a Redox Sensitive Pseudophosphatase. Nature Communications 2020, 11 (1).